Bond behaviour of concrete elements strengthened with NSM CFRP laminate strips under wet-dry cycles

J. Sena-Cruz, P. Fernandes, P. Silva, J. Barros & M. Coelho
ISISE, University of Minho, Department of Civil Engineering, Guimarães, Portugal

J. Xavier
CITAB, University of Trás-os-Montes e Alto Douro, Department of Engineering, Vila Real, Portugal

ABSTRACT: In the last years, the near-surface mounted (NSM) technique has been adopted to increase the load carrying capacity of concrete members. Up to now, research was mainly focused on the structural aspects of NSM strengthening of concrete structures. From an extensive bibliographic search performed, no significant information was found concerning to the NSM long-term performance. The present work has the main objective to contribute for the knowledge on durability performance of the NSM technique with CFRP laminates submitted to wet-dry cycles by means of direct pullout tests. The influence of the bond length, the groove width and depth, and the number of wet-dry cycles on the bond performance were the main parameters analyzed. Thirty five cubic specimens were tested. Digital image correlation method was used, as a complementary tool for monitoring the NSM pullout tests. The tests are described, and the obtained results are presented and discussed.

1 INSTRODUCTION

In the last years, the near-surface mounted (NSM) technique system has been adopted to increase the load carrying capacity of concrete members. In most existing studies, carbon (C) or glass (G) fiber reinforcement polymer reinforcements (FRP) have been used with different cross-sectional shapes (e.g., round, square, rectangular and oval bars, as well as strips). According to the NSM technique, FRP's are introduced into saw cut grooves opened on the concrete cover of the elements to be strengthened. Typically, these grooves are filled with an epoxy adhesive, working as bond agent between FRP and concrete.

Up to now, research was mainly focused on structural aspects of NSM strengthening, like bond behaviour, flexural and/or shear strengthening and beam–column joints strengthening (De Lorenzis & Teng 2007).

When compared with other strengthening techniques, e.g. the externally bonded reinforcement (EBR), the existent knowledge on the NSM reinforcement is much more limited, and several areas still require deeper knowledge. One critical area is the NSM durability and long term behaviour.

The most common environmental conditions for studying the durability are (*fib* 2007): wet-dry cycles in the presence of salts, freeze-thaw cycles, thermal and moisture cycles at fixed temperature and cycles of salt fog. Literature treating the NSM technique

durability is still very scarce and only a few works can be found.

Burke (2008) conducted experimental tests to investigate the performance of flexural NSM FRP strengthening systems applied to reinforced concrete slab strips with $1520 \times 250 \times 100$ mm^3. Specimens were tested under one of three exposure conditions: constant room temperature (21 °C), constant low temperature (-26 °C), and high temperatures (100 °C and 200 °C). Two unstrengthened reference (control) slabs were used for -26 °C and 21 °C environments. The specimens submitted to -26 °C and 21 °C constant temperatures were tested in four-point bending under monotonic loading up to failure. The slabs subjected to high temperatures were tested under a constant load of 20 kN, while the temperature has increased at approximately 10 °C/min up to the predefined threshold maximum temperature, 100 °C or 200 °C. This predefined temperature was kept constant up to failure. The typical failure mode was the debonding at epoxy/concrete interface. The slabs submitted to 100 °C and 200 °C were capable of supporting the load during approximately 43 min. and 11 min., respectively.

Mitchell (2010) carried out freeze-thaw studies with flexural slabs with $1524 \times 254 \times 102$ mm^3 and pullout specimens with geometry similar to the one proposed by De Lorenzis et al. (2002). All elements were strengthened with CFRP strips applied according to the NSM technique. The slabs and pullout specimens were submitted to 300 and 150 freeze-

thaw cycles, respectively. Each cycle consisted on submitting the specimens to -30 ºC during 5 hours, followed by a period of time of 70 min. at +20 ºC. During the heating phase (from -30 ºC to +20 ºC) from the temperature of 0 ºC up to +20 ºC, the specimens were wetted with hot water.The slabs subjected to this environmental conditions showed only a reduction in ultimate load of 2% compared to the reference slabs, and the pullout bond tests showed a reduction of 27%. The main failure mode observed in slabs was debonding at epoxy/concrete interface. In pull-out specimens, the failure occurred due to concrete debonding along the bond length. From the obtained results, the author concluded about the necessity of performing additional studies in this issue.

The main objective of the present work is to contribute to the knowledge on durability performance of the NSM technique with CFRP laminates submitted to wet-dry cycles by means of direct pullout tests. The main parameters analysed were the groove width and depth, and the number of wet-dry cycles on the bond performance. Loaded end slip and pullout force were monitored during pullout tests by the use of a LVDT and a load cell, respectively. Digital image correlation was also used, as complementary method for monitoring the pullout tests. In this paper, those tests are described and the obtained results are presented and discussed.

2 EXPERIMENTAL PROGRAM

2.1 Specimens and test configuration

The experimental program was composed of thirteen series, each one containing two or three specimens. In the context of the present work the influence of the following parameters on the bond performance is assessed: bond length (L_b), groove width (W_g) and depth (D_g), and number of wet-dry cycles. The code name given to the test series consisted on alphanumeric characters separated by underscores (see Table 1). The first string indicates the bond length in millimetres (e.g. Lb60 represents a specimen with a bond length of 60 mm). The second string defines the groove width in millimetres (4 or 8 mm, W4 and W8, respectively). The third string indicates the groove depth (D15 and D25 for the cases of 15 and 25 mm, respectively). The last string refers to the number of wet-dry (WD) cycles that were applied to the specimens. Reference specimens (REF), were kept in a climatic chamber at 20 ºC and 55% of relative humidity, and they were tested at the same time of the corresponding wet-dry series.

Each wet-dry cycle lasted for 24 hours, being the specimens submitted to wetting during 12 hours in water with 3% of NaCl at 20ºC of temperature, followed by 12 hours of drying at about 25ºC.

The period of time between the strengthening and the beginning of the ageing cycles, i.e. the epoxy curing period, was about 150 and 600 days for the D25 and D15 series, respectively. During this time the specimens were kept in laboratory environment.

Figure 1 shows the geometry and test configuration of the pullout direct tests. The specimens' geometry consisted of concrete cubic blocks of 200 mm edge. To avoid premature failure due to the formation of concrete fracture cone at the loaded end, bond lengths started 100 mm from the top.

Table 1. Experimental program.

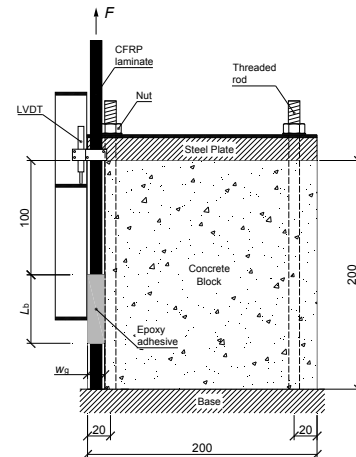| Series	L_b	W_g	D_g	N. of
	mm	mm	mm	Specimens
Lb60_W4_D15_WD90		4		3
Lb60_W4_D15_REF90		4		3
Lb60_W8_D15_WD90	60	8		2
Lb60_W8_D15_REF90		8	15	2
Lb90_W4_D15_WD90		4		3
Lb90_W4_D15_REF90	90	4		3
Lb60_W4_D25_WD90		4		3
Lb60_W4_D25_REF90		4		3
Lb60_W8_D25_WD90	60	8		2
Lb60_W8_D25_REF90		8	25	2
Lb90_W4_D25_WD90		4		3
Lb90_W4_D25_REF90	90	4		3
Lb60_W4_D25_REF250	60	4	25	3

Figure 1. Specimen geometry and test configuration. Note: all units in millimetres.

A steel plate with 20 mm thick was placed at the top of the concrete block to assure negligible vertical displacements at the top of the concrete specimen during pullout test. Four M10 threaded rods fixed this steel plate to the base. A torque moment of 30 N×m was applied to fasten these rods. This torque moment induced an initial compressive state on the concrete block of about 2.0 MPa.

The instrumentation of the specimens consisted of one variable differential transducer (LVDT) and a load cell. The LVDT recorded the relative displacement between the concrete and the CFRP laminate at the top of the concrete block (100 mm apart from the loaded end section). The tests were controlled by another LVDT placed between the actuator and the grip, at rate of 5 µm/s. The applied force, F, was registered by a load cell placed between the grip and the actuator. The overall layout of the performed tests is depicted in Figure 2.
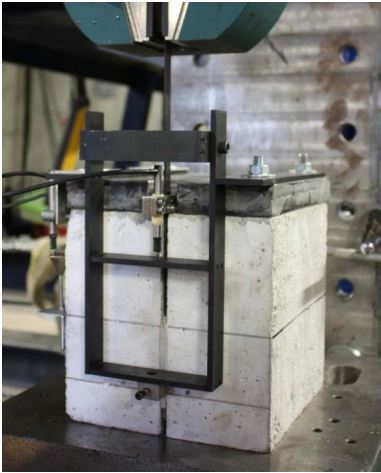

Figure 2. Pullout test setup.

2.2 Digital image correlation method

In addition to the previously referred instrumentation, three specimens (Lb60_W4_S2_REF250 series) were monitored using digital image correlation method.

The digital image correlation (DIC) method provides full-field displacements on quasi-planar objects by maximizing the similarity of features in images corresponding to different deformation states (Pan et al. 2009). Conventionally, adjacent square subsets are defined in the reference image (undeformed configuration) by a given number of pixels. By mathematical correlation of these patches on a pair of images, taken before and after deformation, a displacement vector is determined per subset. Therefore, the subset size defines the displacement spatial resolution associated to the measurements and must be chosen in a compromise between correlation and interpolations errors.

The target surface must have a local, random (isotropic) and contrasted gray level distribution suitable for solving the correspondence problem in image processing. In this case, such textured pattern was created across the concrete surface by painting. The surface was previously uniformed using iron paste

and polished afterwards with 300-grit sandpaper. White matte background paint was firstly applied on the region of interest, followed by a spread distribution of black painting using aerosol spray. The typical speckle pattern obtained with this marking technique is shown in Figure 3.
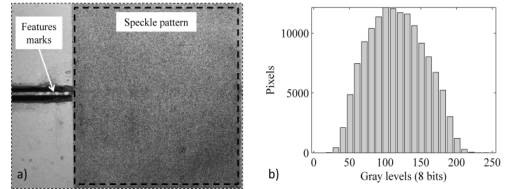

Figure 3. (a) Specimen feature and speckle patterns; (b) Histogram of the speckle pattern used in the digital image correlation.

The GOM ARAMIS® DIC-2D v6.02 software (ARAMIS 2012) was used in this work. The optical system was equipped with an 8-bit Charged-Coupled Device (CCD) Baumer Optronic FWX20 camera (resolution of 1624×1236 pixels, pixel size of 4.4 µm and sensor format of 1/1.8"), coupled with an Nikon Zoom Nikkor AF 28-105mm f/3.5-4.5D IF lens (see Figure 4). Images were recorded with an acquisition frequency of 0.2 Hz. The lens aperture was set to f/11 for enhancing depth of field and avoiding diffraction effects (smallest apertures).
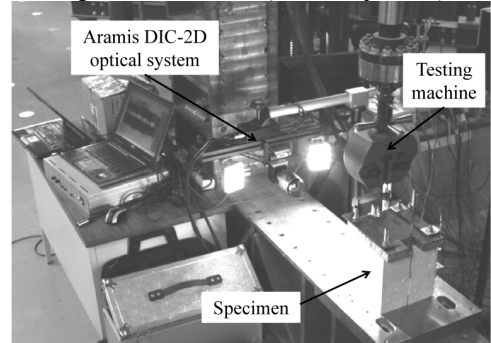

Figure 4. Photo-mechanical experimental setup.

Lighting intensity and shutter time were adjusted in order to obtain a uniform illumination, avoid pixel saturation and prevent motion blur in the images during exposure. The components of the optical system and measurement parameters used in this work are summarized in

Table 2. The facet size (number of pixels per subset) and the facet step (distance between adjacent facet centres) were set to 15×15 pixels². This subset size was found a suitable compromise, attending to the size of the region of interest, the optical system (magnification) and the quality of the speckle obtained by spray painting. The in-plane displacements

were then numerically differentiated in order to determine the strain field by using a computation size of 7 subsets (Table 2). The displacement and strain resolution associated to the DIC measurements are, respectively, in the range of 2×10^{-2} pixel and 0.02% (ARAMIS 2012, Xavier et al. 2012).

Table 2. Optical system components and measurement parameters

CCD Cameras	
Model	Baumer Optronic FWX20 (8 bits, 1624×1236 pixels)
Shutter time	3 ms
Frequency	0.2 Hz
Lenses:	
Model	Nikon Zoom Nikkor AF 28-105mm f/3.5-4.5D IF
Aperture	f/11
Lighting	Raylux 25 white-light LED
Working distance	470 mm
Conversion factor	0.033 mm/pixel
ARAMIS DIC-2D	
Facet size	15×15 pixels^2
Step size	15×15 pixels^2
Strain step	7 subsets
Measuring points	15×15 pixels^2

2.3 *Material characterization*

Prior to the ageing cycles, mechanical material characterization of the concrete, CFRP laminate and epoxy adhesive was performed.

The mechanical characterization of the concrete was assessed by means of compression tests. For that purpose cylindrical concrete specimens with a diameter of 150 mm and a height of 300 mm were tested for a concrete age of 28 days to evaluate the compressive strength according to the NP EN 12390-3:2009. The results indicated an average compressive strength of 26.37 MPa, with a coefficient of variation (CoV) of 4.0%. Only one batch was used to cast all the concrete specimens used in the pullout tests.

The CFRP laminate utilized in the present work, with a cross section of 1.4 mm thick and 10 mm wide, and a trademark CFK 150/2000, was provided in rolls of 100 meters each, and was supplied by S&P® Clever Reinforcement Company. This laminate is composed of unidirectional carbon fibres agglutinated by an epoxy adhesive, and has a smooth external surface. Tensile properties of the CFRP were assessed by performing tensile tests according to ISO 527-5 (1997), and adopting a displacement rate of 2 mm/min. To evaluate the modulus of elasticity, a clip gauge was mounted at middle region of each specimen. From the mechanical characterization, a modulus of elasticity, a tensile strength and a strain at peak stress of, respectively, 158 GPa (0.9%), 2435 MPa (CoV=5.8%) and 1.50% (CoV=4.7%) were obtained. Practically for all the specimens the failure mode occurred in explosive fa-

shion due to the fibre progressive rupture at mid-height (Sena-Cruz et al. 2011).

Tensile tests were conducted to evaluate the mechanical properties of the epoxy adhesive according to the ISO 527-2 (1993). To determine the modulus of elasticity, a clip gauge was mounted at middle region of each specimen. From the tensile tests, a tensile strength of 17.33 MPa (CoV=5.8%) and modulus of elasticity of 6.35 GPa (CoV=5.8%) were obtained.

2.4 *Preparation of the specimens*

The preparation of the strengthened specimens required several steps, mainly cutting the grooves, cleaning the grooves and FRP surfaces, adhesive preparation and strengthening. For both series (D15 and D25), the CFRP strip was located at the middle of the groove.

3 RESULTS

3.1 *Materials*

Mechanical properties of the CFRP laminate and epoxy adhesive were assessed after being submitted to 90 dry-wet cycles in the same conditions of the corresponding pullout specimens.

A tensile strength of 2281.71 MPa (CoV=5.81%) and a modulus of elasticity of 154.66 GPa (CoV=4.05%) were obtained for the laminate. When this values are compared with those of the reference specimens, a decrease of 6.3% and 2.1% are obtained for the tensile strength and modulus of elasticity, respectively.

On the other hand, for the case of the epoxy adhesive a tensile strength of 15.65 MPa (CoV=22.2%) and a modulus of elasticity of 5.87 GPa (CoV=17.1%) were obtained. Comparing these values with the corresponding reference specimens (see section 2.3) a decrease of 9.7% and 7.6% for the tensile strength and modulus of elasticity was obtained, respectively, and the CoV of both properties has increased significantly.

3.2 *Pullout tests*

Table 3 presents the main results obtained for the tested series in terms of maximum pullout force, F_{lmax}, and corresponding loaded end slip, s_{lmax}, the average bond stresses $\tau_{max,av1}$ and $\tau_{max,av2}$, and failure modes.

The evaluation of the loaded end slip was calculated from the values recorded by the LVDT (see Figure 1). The records registered by the LVDT include the loaded end slip, s_l, and the elastic deformation of the CFRP between the loaded end section and the top surface of the concrete block (100 mm of distance).

In the present analysis the elastic deformation was removed, therefore only the s_l is considered. For that purpose the modulus of elasticity of 158 GPa was used (see Section 2.3). The $\tau_{max,av1}$ and $\tau_{max,av2}$ are the average bond stress at the CFRP-epoxy and concrete–epoxy interfaces, respectively, and are evaluated by $F_{fmax}/(P_f L_b)$ and $F_{fmax}/(P_g L_b)$, being P_f the perimeter of the CFRP cross-section and P_g the perimeter of the groove cross-section in contact with the adhesive.

Three distinct failure modes occurred (see Figure 5): concrete splitting (C), CFRP failure (F) and debonding at adhesive/laminate interface (D). Concrete splitting was characterized by a large area of detached concrete surrounding the bonded region. This type of failure mode was observed mainly in the D15 series, i.e. with the laminate closer to the external concrete surface. Debonding at adhesive/laminate interface was mainly observed in the D25 series. In general, this failure mode did not generate any type of crack in concrete and/or in adhesive. The CFRP failure occurred at the loaded end section. Partial or total collapse of the CFRP cross-section has characterized this type of failure mode.
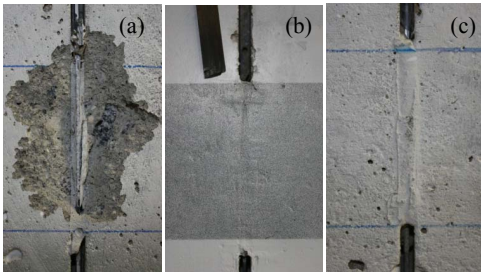

Figure 5. Failure modes: (a) Concrete splitting; (b) CFRP failure; (c) Debonding at adhesive/laminate interface.

For better understanding the evolution of maximum pullout force obtained in the experimental program, Figure 6 is depicted. In this figure the strengthen variation is defined as the ratio between $F_{lmax,WD} - F_{lmax,REF}$ and $F_{lmax,REF}$ being "WD" and "REF" a generic series submitted to wet-dry cycles and the corresponding reference series, respectively.

Figure 6 shows that in series D15 the ageing effect has decreased F_{lmax}, regardless the bond length and the width of the groove, while in series D25, apart W8, the F_{lmax} has increased with the ageing. This paradoxical behaviour may be explained by the curing period used for the two series. As referred before, the epoxy curing period was about 600 and 150 days for the D15 and D25 series, respectively. The adopted period of time for the latter one may have not been sufficient to assure the complete cure, before starting the ageing tests, resulting a positive balance in terms of bond performance due to curing and ageing effects provided by the ageing conditions.

This aspect could also contribute for the failure modes observed, since for the D15 series the most common was the concrete splitting whereas the adhesive/laminate interface debonding has governed the D25 series (see also Figure 5).

Apparently, the series with a groove width of 8 mm (W8) were not affected by the period of time of the epoxy adhesive neither the wet-dry cycles. As referred before, for the D25 series the adhesive plays an important role, being higher for the case of W8, when compared with W4. Due to the ageing effects, the performance of the former series was significantly affected by the degradation agents. In the D15 series the type of failure mode changed from C (in W4 series) to D (in series W8) due to P_g.

As expected, the pullout force has increased with both the bond length and groove depth.

Table 3. Experimental results (average values).

Series	F_{lmax}	s_{lmax}	$\tau_{max,av1}$	$\tau_{max,av2}$	Failure
	kN	mm	MPa	MPa	mode
Lb60_W4_D15_WD90	25.34 (5.88%)	0.37 (23.56%)	18.52	12.42	C(3)*
Lb60_W4_D15_REF90	29.00 (2.67%)	0.61 (23.10%)	21.20	14.22	C(3)*
Lb60_W8_D15_WD90	26.08 (0.81%)	0.81 (1.75%)	19.06	11.44	D+C(2)*
Lb60_W8_D15_REF90	26.83 (0.55%)	0.88 (25.05%)	19.61	11.77	D(2)*
Lb90_W4_D15_WD90	32.44 (10.10%)	0.79 (51.93%)	15.81	10.60	C(2)*; F(1)*
Lb90_W4_D15_REF90	36.39 (5.31%)	1.06 (8.71%)	17.73	11.89	C(2)*
Lb60_W4_D25_WD90	31.14 (3.16%)	0.54 (15.85%)	22.76	9.61	D(3)*
Lb60_W4_D25_REF90	28.04 (8.63%)	0.47 (7.67%)	20.50	8.65	D(3)*
Lb60_W8_D25_WD90	30.24 (2.97%)	0.74 (34.40%)	22.11	8.69	D(2)*
Lb60_W8_D25_REF90	30.63 (0.35%)	0.71 (9.96%)	22.39	8.80	D(2)*
Lb90_W4_D25_WD90	35.10 (18.68%)	0.91 (18.40%)	17.11	7.22	C(3)*
Lb90_W4_D25_REF90	32.60 (16.77%)	0.70 (57.99%)	15.89	6.71	F(1)*; D(1)*
Lb60_W4_D25_REF250	25.64 (9.91%)	0.73 (12.94%)	18.74	7.91	D(1)*; F(2)*

Note: the values in parentheses are the corresponding coefficients of variation; Failure modes: D=Debonding at adhesive/laminate interface; F=CFRP failure; C=Concrete splitting; *the value between parenthesis is the number of specimens with this type of failure mode.
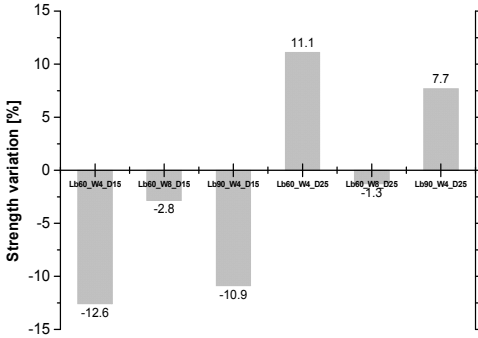
Figure 6. Strength variation.

Figure 7 shows typical responses in terms of pullout force *versus* loaded end slip (F_l–s_l), which is an eminently non-linear relationship up to failure.
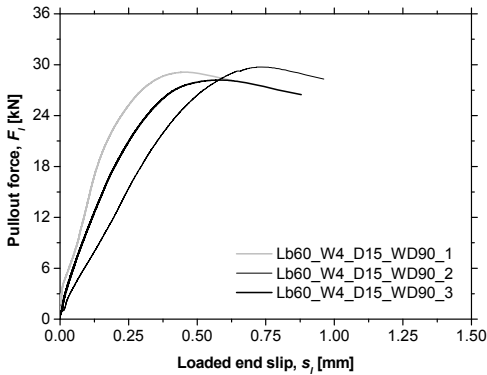

Figure 7. Pullout force *versus* loaded end slip for the Lb60_W4_D15_WD90 series.

3.3 *Digital image correlation method*

As referred before, in the ambit of the present experimental program the digital image correlation was tested as an alternative/complementary method for monitoring NSM pullout tests. For that purpose the series Lb60_W4_D25_REF250 was used. In the context of the present paper, the results obtained for the first specimen of this series are present and analysed in this section. Figure 9 shows for different levels of pullout force the following parameters: deformed specimen; displacements U_x and U_y in the x and y axis, respectively; the strain field in x and y direction (ε_x and ε_y); and, the distortional field xy (γ_{xy}). In the figures obtained from DIC the loaded section of the CFRP laminate corresponds to the left extremity of these figures. Axis x was assumed parallel to the longitudinal axis of the laminate, i.e. in the direction of the pullout force.

A comparison between the measured loaded end slip using the LVDT and the DIC method is depicted in Figure 8, in terms of pullout force versus loaded end slip. Due to some misalignment of the laminate, in the first phase of the slippage the laminate has also rotated in order to be aligned with the loading direction, resulting a negative slip that is the main cause of the difference in the F_l-s_l obtained from the two methods. This behaviour was clearly captured by the LVDT with an initial negative slip. On the other hand, the DIC method did not capture this behaviour, since the version used in present work only measure 2D deformations. In spite of that, the overall behaviour is very similar.
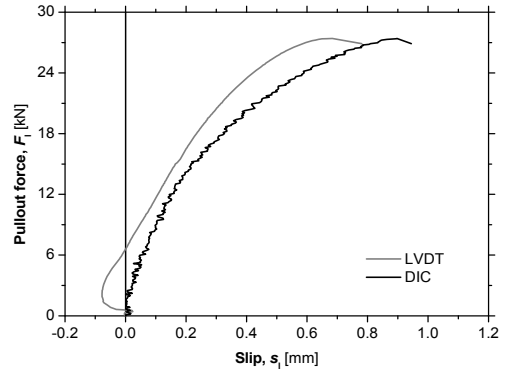

Figure 8. Pullout force *versus* loaded end slip using a LVDT and the DIC method to measure the loaded end slip.

The evolution of the maximum U_x displacements occurred in each step is clearly observed by DIC method. At the maximum pullout force level, the maximum U_x displacement was about 0.035 mm in the debonding region. As expected, higher displacements occurred in the groove region.

Like U_x, the U_y displacements were symmetric in relation to the longitudinal axis of the laminate, being the maximum level of deformation about 0.015 mm at the peak load. When the magnitude of U_x and U_y displacements are compared, the former is approximately 10 times higher.

The recorded strains measured by the DIC method put in evidence the resistant mechanism reported in the literature (Sena-Cruz & Barros 2004). Diagonal compressive forces (struts) are developed in the adhesive and then are transferred to concrete. This behaviour is clearly observed by the DIC, as well as by the yield the "fish spine" crack pattern observed on the epoxy adhesive (see Figure 5a and also Figure 9). Another interesting aspect is the fact that the maximum strains occurred for F_{lmax} at the vicinity of the free end region with strain level ε_x similar to ε_y.
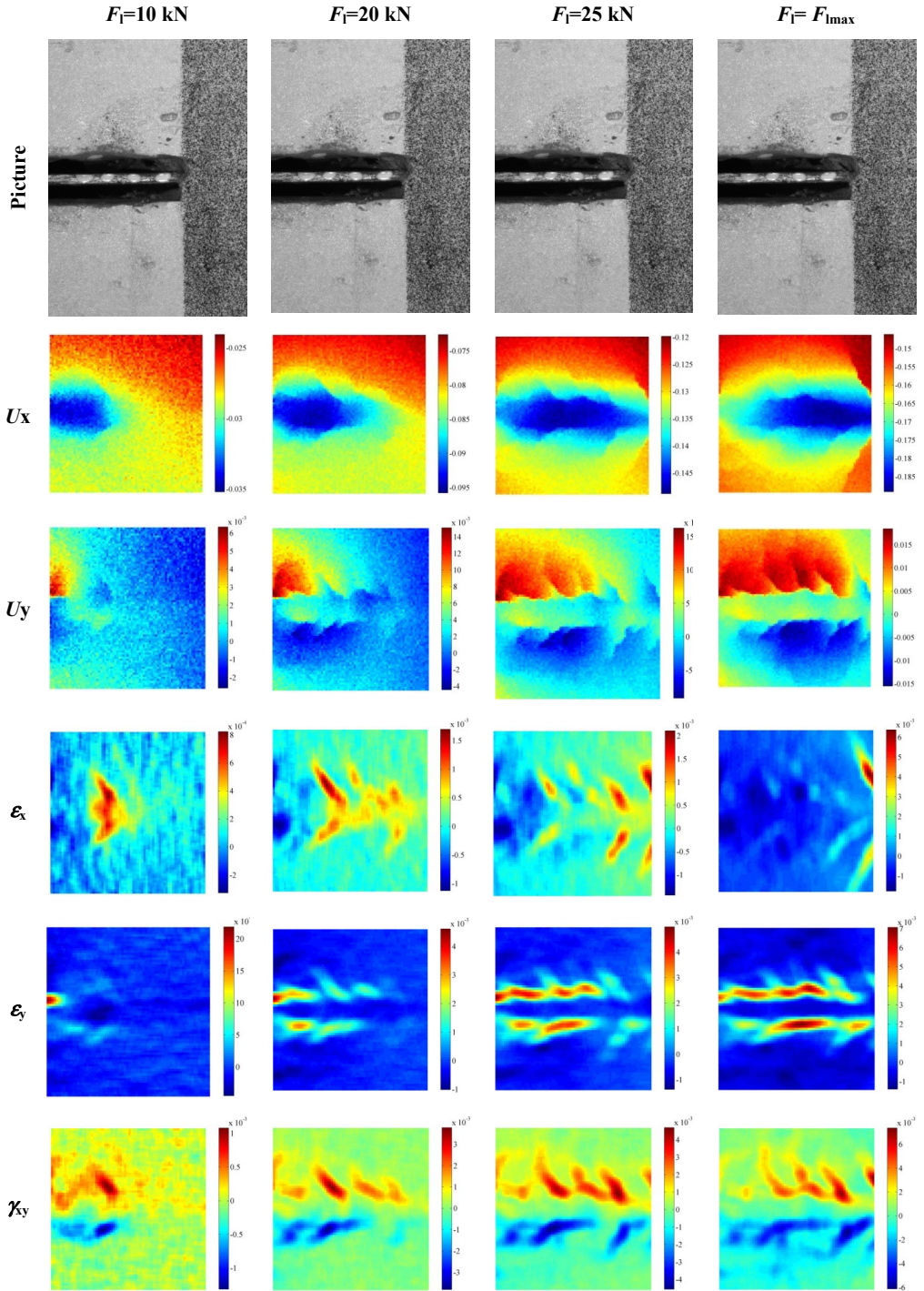
1028

Figure 9. Results obtained using the DIC method for distinct levels of pullout force.

4 CONCLUSIONS

This work presented the main results obtained from an experimental program with pullout tests of concrete elements strengthened with NSM CFRP laminate strips, after being submitted to 90 wet-dry cycles. In this experimental work the influence of two different groove depths (15 mm and 25 mm), bond lengths (60 mm and 90 mm) and strengthening application ages (150 and 600 days) on the bond performance was studied.

From the results obtained, a decrease in the maximum pullout force, F_{lmax}, of about 11% was observed for the series with grooves of 15 mm depth and 4 mm wide, when compared to the reference specimens. On the other hand, an increase of about 10% for the F_{lmax} was found in the series with grooves of 25 mm depth and 4 mm wide. Negligible variation was encountered for the F_{lmax} in the series with grooves of 8 mm wide, when compared with the corresponding reference series.

In spite of the present results being credible and contributing for the knowledge in this area, further investigation is required to better understand the observed phenomena.

In the ambit of the present experimental program the digital image correlation (DIC) was tested as an alternative/complementary method for monitoring NSM pullout tests revealing to be a useful tool for this type of purpose.

REFERENCES

ARAMIS commercial software. GOM (http://www.gom.com/). <2012-01-26>

Burke, P.J. 2008. Low and High Temperature Performance of Near Surface Mounted FRP Strengthened Concrete Slabs. Master of Science, Queen's University.

De Lorenzis, L. & Teng, J.G. 2007. Near-surface mounted FRP reinforcement: An emerging technique for strengthening structures. *Composites Part B: Engineering* 38 (2): 119-143.

De Lorenzis, L., Rizzo, A. & La Tegola, A. 2002. A modified pull-out test for bond of near-surface mounted FRP rods in concrete. *Composites Part B: Engineering* 33 (8): 589-603.

fib 2007. FRP reinforcement in RC structures. Bulletin No. 40. The International Federation for Structural Concrete (FIB). Report prepared by Task Group 9.3, ISBN: 978-2-88394-080-2. 160 pp. Lausanne, Switzerland.

ISO 527-2 1993. Plastics – Determination of tensile properties – Part 2: Test conditions for moulding and extrusion plastics. *International Organization for Standardization* (ISO): 5pp. Genève, Switzerland.

ISO 527-5 1997. Plastics – Determination of tensile properties – Part 5: Test conditions for unidirectional fibre-reinforced plastic composites. *International Organization for Standardization* (ISO): 9pp. Genève, Switzerland.

Mitchell, P.A. 2010. Freeze-Thaw and Sustained Load Durability of Near Surface Mounted FRP Strengthened Concrete. Master Thesis, Queen's University.

NP EN 12390-3. 2009. Ensaios de betão endurecido. Parte 3: Resistência à compressão de provetes de ensaio. *Instituto Português da Qualidade* (IPQ): 21 pp. Lisbon, Portugal. [in Portuguese].

Pan, B., Qian, K., Xie. H. & Asundi, A. 2009. Two-dimensional digital image correlation for in-plane displacement and strain measurement: a review. *Measurement Science and Technology* 20(6), 062001.

Sena Cruz, J.M. & Barros, J.A.O. 2004. Bond Between Near-Surface Mounted Carbon-Fiber-Reinforced Polymer Laminate Strips and Concrete. *Journal of Composites for Construction*, 8 (6): 519-527.

Sena Cruz, J.M., Barros, J.A.O., Coelho, M.R., Silva, L. 2011. Efficiency of different techniques in flexural strengthening of RC beams under monotonic and fatigue loading. *Construction & Building Materials*, 29: 175–182.

Xavier, J., de Jesus, A.M.P., Morais, J.J.L. & Pinto, J.M.T. 2012. Stereovision measurements on evaluating the modulus of elasticity of wood by compression tests parallel to the grain. *Construction and Building Materials*, 26 (1): 207–215.